Hindawi
Advances in Civil Engineering
Volume 2019, Article ID 1251295, 15 pages
https://doi.org/10.1155/2019/1251295

Research Article

Calculation Method of Seismic Residual Displacement of Sheet Pile Quay Walls

Liyan Wang,[1] Zhou Yajun,[2] Wenxue Gong,[3] Jinsong Li,[3] and Aimable Ishimwe[4]

[1]*Professor (PhD), School of Civil and Architectural Engineering, Jiangsu University of Science and Technology, No. 2 Mengxi Road, Zhenjiang, Jiangsu Province, China*
[2]*Senior Engineer (Ma.), Jiangsu Surveying and Design Institute of Water Resources Co., Ltd., Yangzhou, Jiangsu Province, China*
[3]*Master Student (Ba.), School of Civil and Architectural Engineering, Jiangsu University of Science and Technology, No. 2 Mengxi Road, Zhenjiang, Jiangsu Province, China*
[4]*School of Civil and Architectural Engineering, Jiangsu University of Science and Technology, No. 2 Mengxi Road, Zhenjiang, Jiangsu Province, China*

Correspondence should be addressed to Liyan Wang; wly_yzu@163.com

Received 28 April 2019; Accepted 17 June 2019; Published 1 August 2019

Academic Editor: Giovanni Minafò

Sheet pile quay walls have widely been used in port engineering, hydraulic engineering, and civil engineering, but the sheet pile quay is a flexible retaining structure, which undergoes large deformation during earthquakes. The seismic design methods of the sheet pile quay wall in different countries are greatly different, and there is deficit of studies performed on the seismic residual displacement of the sheet pile quay walls. Based on the pseudostatic method and the calculation method for obtaining the dynamic earth pressure of clay soil, it is assumed that the cantilever part of the sheet pile quay wall bears the dynamic active earth pressure and the part in deep soil bears dynamic passive earth pressure on the side of the sea and bears dynamic active earth pressure on the side of the ground. The hydrodynamic pressure acting in front of the wall is calculated using Westergaard's approach. The displacement of the front wall of the sheet pile quay is calculated, respectively, according to the upper part and lower part of mud surface. Based on the deflection curve differential equation and boundary conditions, the calculating formulas on seismic residual displacements of the sheet pile quay walls are derived and the proportional displacement method for determining the tension force of the pull rod is given. Combining with an engineering case, the theoretical calculation results are compared with the ADINA simulation results, and comparison results show that these two calculation methods are close under the mud, but they have little difference in the calculation results of the part above the mud because of the proportional displacement method of the tension force of the pull rod.

1. Introduction and Background

1.1. Introduction. Sheet pile quay walls have widely been used in coastal and inland areas with many advantages that include simple structure, low material consumption, low cost, and the main component can be prefabricated in the factory. It not only bears general actions in design but also bears seismic actions and can be destroyed due to improper design during earthquakes [1]. For example, during Kobe Hyogo-ken earthquake in Japan, the sheet pile quay walls were severely damaged, and the steel plates were fractured (2001). It is necessary to study the stress and deformation of the sheet pile quay structure under earthquakes [2].

Due to the lack of corresponding observations and model tests on seismic response of sheet pile quay walls, and some simple and practical methods in some general standards, and due to the difference in experience, science technology, and economy, the seismic design methods of the sheet pile quay wall in different countries are greatly different. Therefore, it is important to study theoretical calculation methods of seismic displacements of the front walls in sheet pile quays.

1.2. Background. Several theories and findings on the seismic analysis of sheet pile wharves have been developed over the last several decades through experiments with shaking table tests [3–5]. The real control factor of the seismic safety of a geostructure is its deformation rather than its strength. It is gradual to become a development trend for evaluating seismic characters of geotechnical structures applying deformation as a control criterion (2005). At the present, there are many studies on the sheet pile quay wall with specific content as follows: Lee and Chang [6] proposed a procedure of damage inspection for the infrastructure in the harbor, which is a two-stage inspection strategy. Choudhury pertains to a study in which the effect of earthquakes along with the hydrodynamic pressure including inertial forces on such a retaining wall is observed. The hydrodynamic pressure is calculated using Westergaard's approach, while the earth pressure is calculated using Mononobe–Okabe's pseudo-static analysis [7]. Tan and Lu [8] presented a thorough finite element (FE) parametric study of sheet pile wall deflections caused by deep dynamic compaction (DDC). Motamed and Towhata [9] presented experimental results of a series of 1 g shake table tests on mitigation measures for a model consisting of a 3×3 pile group and a sheet pile quay wall.

The FEM software ANSYS is used for the analysis of the interaction of steel sheet pile and soil model in Wang Xi's study, then the two conditions of steel sheet pile when it is normal and corroded have been simulated, and the force status of the steel sheet pile and distortion of link-banked structure and soil were obtained. It can provide evidence for judging steel sheet pile safety [10]. Bilgin [11] presented the results of the numerical parametric study performed and comparative analyses of the anchored sheet pile walls constructed by the finite element method. A series of calculation distribution figures in the paper can be applied to initially predict the seismic residual deformation of quay walls for engineering designers [12].

A pseudodynamic method for calculating the seismic residual deformation was provided, and the rationality and the reliability of the prediction method are validated by a 1 g shaking table model test and a 120 g centrifuge shaking table model test [13]. The author studied the dynamic response of reinforced earth retaining walls under earthquake action [14, 15] and proposed a calculation method for residual deformation [16], prediction method of seismic residual deformation of caisson quay walls in liquefied foundation [17], and displacement calculation method of front wall of covered sheet pile wharves [18]. Chiou et al. [19] proposed a procedure for developing seismic fragility curves for a pile-supported wharf. Based on the damage criteria and the response matrix, the fragility curves of the wharf can thus be constructed through simple statistical analysis. Shifted lognormal cumulative distribution functions are also employed to better approximate the fragility curves for practical applications. Cheng et al. [20] revealed that the composite steel sheet pile wall can exert the greater global bending stiffness and reduce the lateral soil pressure by the two-dimensional numerical simulations. Of course, the improvement treatment of backfill soils is an important method to reduce the displacement on sheet pile quay walls. The improvement of backfill soils includes many methods, and the authors in the paper have carried out some research on the improvement of backfill soils [21, 22].

In this paper, based on the graphical method conducted by Lin et al. [23] in obtaining the dynamic soil pressure of clay soil, considering structural characteristics of sheet pile quay walls and differential equation of the deflection curve, some calculating formulas on the seismic residual displacement of the front walls in the sheet pile quays are derived. A comparison is made between the theoretical calculation results and the ADINA simulation results to prove the effectiveness of the theoretical equation.

2. Dynamic Earth Pressure of Cohesive Soil

2.1. Calculation Model. The sheet pile quay wall has the tendency of sliding failure, while the top displacement of the front wall is large, and the bottom displacement is small under earthquakes. The wall has the tendency to rotate around the bottom, and when the wall displacement reaches a certain value along the direction from the soil under earth pressure, the backfill behind the wall slides along the back of the wall and through a plane called BC of soil where the angle between the wall base and the vertical plane is θ. This part of the soil is called sliding wedge OBC. The earth pressure of the front wall is caused by the sliding wedge of OBC, and the calculation model is shown in Figure 1. The wall is vertical and rough; $\delta, c, \varphi, \theta, q, P_E$, and W are represented as the friction angle of the wall, cohesive force of soil after wall, internal friction angle, the dip angle of the soil surface after the wall, surface uniform load, the total seismic active earth pressure force under seismic load, and sliding wedge gravity, respectively. $k_h W$ and $k_v W$ are horizontal and vertical seismic loads of sliding wedge, R_a is the tension force of the pull rod, R is the reaction force on BC, C is the total cohesion on BC, C_w is the total adhesion on OC, P_{stu} is the hydrostatic pressure, and P_{dyn} is the hydrodynamic pressure.

Based on the research on the graphical method for obtaining the dynamic soil pressure of clay soil in Reference [2], some change has been made in the paper according to characteristics of sheet pile quay walls and has been applied to calculate seismic earth pressures of sheet pile quay walls.

2.2. Acting Position of Seismic Total Earth Pressures on the Back of Sheet Pile Quay Wall. Schematic diagrams of seismic total active earth pressure calculation and forces acting on a horizontal microelement soil mass are shown in Figure 2.

Effective load acting on the O_1B_1 surface is presented as follows:

$$q_1 = q + \gamma h_c. \tag{1}$$

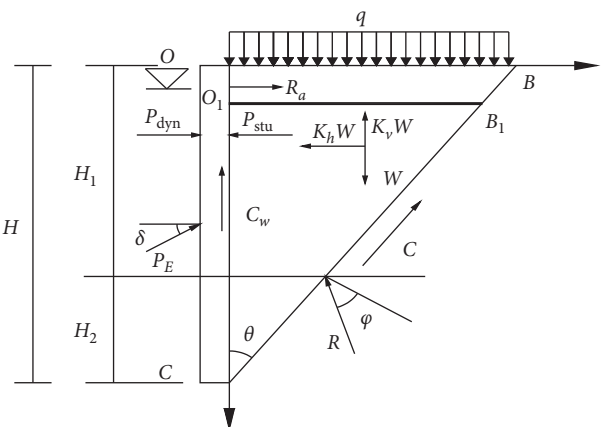

Figure 1: Diagram of the calculation model.

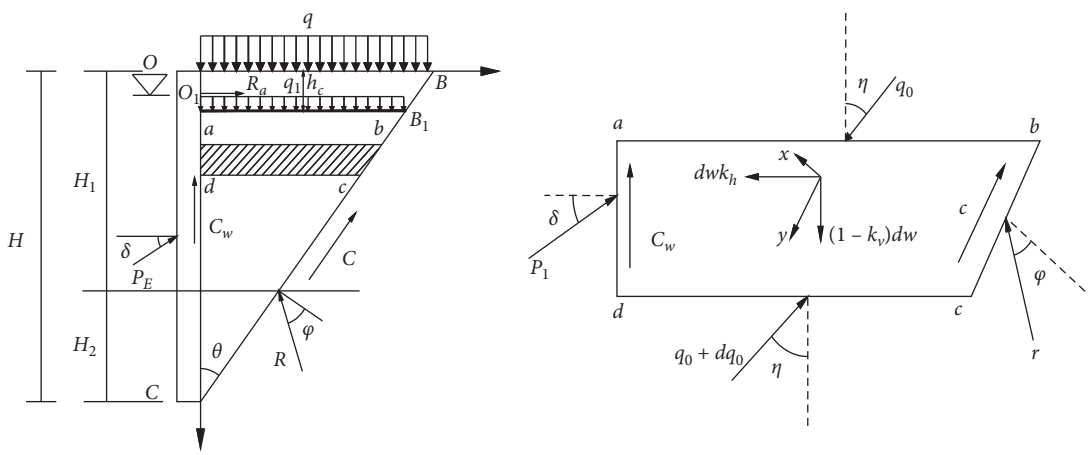

Figure 2: (a) Schematic diagram of seismic total active earth pressure. (b) Forces acting on a horizontal microelement soil mass.

Furthermore,

$$q_0 = \frac{q_1(1-k_v)}{\cos\eta},$$
$$\frac{dq_0}{dh} - \frac{a}{H-h}q_0 = \frac{b}{H-h} + \frac{1-k_v}{\cos\eta}\gamma, \tag{2}$$

where

$$a = 1 - n_1\frac{\cos\theta\sin(\theta+\phi+\delta)}{\cos(\theta+\phi-\eta)\sin\theta},$$
$$b = \frac{2[c_w\sin(\theta+\phi)\cos\delta\cos\theta - c\cos\phi\cdot\sin\delta]}{\sin\theta[\sin\delta\cos(\theta+\phi-\eta)-\sin(\theta+\phi)\cos(\delta+\eta)]},$$
$$n_1 = \frac{\cos(\theta+\varphi-\eta)}{\cos\theta}\cdot\frac{\cos\theta\sin\eta-\sin(\theta-\eta)}{\sin\delta\cos(\theta+\varphi-\eta)-\sin(\theta+\varphi)\cos(\delta+\eta)}. \tag{3}$$

2.2.1. The Position of Active Earth Pressure. The seismic total active earth pressure of cohesive soil could be expressed as

$$\begin{aligned} P_{E1} &= \frac{1}{2}\gamma(H-h_c)^2\frac{1-k_v}{\cos\eta}\frac{\sin\theta\cos(\theta+\varphi-\eta)}{\cos\theta\sin(\theta+\varphi+\delta)} \\ &= c(H-h_c)\frac{\cos\varphi}{\cos\theta\sin(\theta+\varphi+\delta)} \\ &\quad + (q+\gamma h_c)(H-h_c)\cdot\frac{1-k_v}{\cos\eta}\frac{\sin\theta\cos(\theta+\varphi-\eta)}{\cos\theta\sin(\theta+\varphi+\delta)} \\ &\quad - c_w(H-h_c)\frac{\cos(\theta+\varphi)}{\sin(\theta+\varphi+\delta)}. \end{aligned} \tag{4}$$

(1) When $a \neq 0$ and $a \neq -1$, the distance z_1 between the acting point of dynamic active earth pressure joint forces and bottom of the wall under the earthquake is

$$z_1 = \frac{\int_{h_c}^{H} p_1 (H-h) dh}{\int_{h_c}^{H} p_1 dh} = \frac{((m_1 (H-h_c)^{-a})/(2-a)) - ((m_2 (H-h_c))/3) - (m_3/2)}{((m_1 (H-h_c)^{-a})/(1-a)) - ((m_2 (H-h_c))/2) - m_3} (H-h_c). \tag{5}$$

(2) When $a = 0$, the distance z_1 between the acting point of dynamic active earth pressure joint forces and the bottom of the wall under the earthquake is

$$z_1 = \frac{(1/6)((1-k_v)/\cos\eta) n_1 \gamma (H-h_c) + (1/2)((1-k_v)/\cos\eta) n_1 q_1 + (1/4) n_1 b - (1/2) n_2 c_w + (1/2) n_3 c}{(((1-k_v) n_1 \gamma (H-h_c))/2\cos\eta) + ((1-k_v)/\cos\eta) n_1 q_1 + n_1 b - n_2 c_w + n_3 c} (H-h_c). \tag{6}$$

(3) When $a = -1$, the distance z_1 between the acting point of dynamic active earth pressure joint forces and the bottom of the wall under the earthquake is

$$z_1 = \frac{(1/9)((1-k_v)/\cos\eta) n_1 \gamma (H-h_c) + (1/3)((1-k_v)/\cos\eta) n_1 q_1 + (1/6) n_1 b - (1/2) n_2 c_w + (1/2) n_3 c}{(((1-k_v) n_1 \gamma (H-h_c))/4\cos\eta) + (1/2)((1-k_v)/\cos\eta) n_1 q_1 + (1/2) n_1 b - n_2 c_w + n_3 c} (H-h_c). \tag{7}$$

Force analysis of passive earth pressure of horizontal microelement soil mass is shown in Figure 3.

2.2.2. The Position of Dynamic Passive Earth Pressure. Passive earth pressure joint forces of cohesive soil under the earthquake is

$$\begin{aligned} P_{E2} = {} & \frac{1}{2}\gamma H^2 \frac{1-k_v}{\cos\eta} \frac{\sin\theta\cos(\theta+\eta-\phi)}{\cos\theta\sin(\theta-\phi-\delta)} \\ & + qH \frac{1-k_v}{\cos\eta} \frac{\sin\theta\cos(\theta+\eta-\phi)}{\cos\theta\sin(\theta-\phi-\delta)} \\ & + cH \frac{\cos\phi}{\cos\theta\sin(\theta-\phi-\delta)} + c_w H \frac{\cos(\theta-\phi)}{\sin(\theta-\phi-\delta)}. \end{aligned} \tag{8}$$

(1) When $A \neq 0$ and $A \neq -1$, the distance z_2 between the acting point of dynamic passive earth pressure joint forces and the bottom of the wall under the earthquake is

$$\begin{aligned} z_2 &= \frac{\int_0^H p_2 (H-h) dh}{\int_0^H p_2 dh} \\ &= \frac{(m_{p1} H^{-A}/(2-A)) - (m_{p2} H/3) - (m_{p3}/2)}{(m_{p1} H^{-A}/(1-A)) - (m_{p2} H/2) - m_{p3}} H. \end{aligned} \tag{9}$$

(2) When $A = 0$, the distance z_2 between the acting point of dynamic passive earth pressure joint forces and the bottom of the wall under the earthquake is

$$z_2 = \frac{(1/6)((1-k_v)/\cos\eta) n_{p1} \gamma H + (1/2)((1-k_v)/\cos\eta) n_{p1} q + (1/4) n_{p1} B + (1/2) n_{p2} c_w - (1/2) n_{p3} c}{((1-k_v) n_{p1} \gamma H)/2\cos\eta) + ((1-k_v)/\cos\eta) n_{p1} q + n_{p1} B + n_{p2} c_w - n_{p3}} H. \tag{10}$$

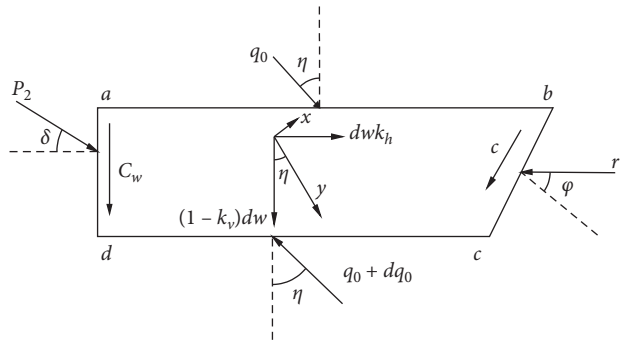

Figure 3: Force analysis of passive earth pressure of horizontal microelement soil mass.

(3) When $A=-1$, the distance z_2 between the acting point of dynamic passive earth pressure joint forces and the bottom of the wall under the earthquake is

$$z_2=\frac{(1/9)\left((1-k_v)/\cos\eta\right)n_{p1}\gamma H+(1/3)\left((1-k_v)/\cos\eta\right)n_{p1}q+(1/6)n_{p1}B+(1/2)n_{p2}c_w-(1/2)n_{p3}c}{\left(\left(n_{p1}\gamma H(1-k_v)\right)/4\cos\eta\right)+(1/2)\left((1-k_v)/\cos\eta\right)n_{p1}q+(1/2)n_{p1}B+n_{p2}c_w-n_{p3}c}H. \tag{11}$$

3. Calculation of the Wall Displacement for Sheet Pile Quay Wall under Earthquakes

3.1. Calculation Mode. The front sheet pile walls produced larger displacement, and the sheet pile structure had the tendency of slope failure under earthquakes; thus, the upper part displacement of the sheet pile wall is larger, and the pattern of slope deformation is presented. Due to the large deformation displacement of the sheet pile wall, it is assumed that the part of the cantilever sheet pile wall bears the dynamic active earth pressure of the soil after the wall, the part of deep soil bears dynamic passive earth pressure of the soil on the side of the sea, and the part of deep sea that can bear dynamic active earth pressure of the soil on the side of the ground. When the deformation of the sheet pile wall was calculated, the sheet pile wall is divided into two parts: one is on the surface and the other is under the surface and both of all were calculated, respectively. The calculation of the part on the surface is shown in the calculation model as Figure 4(a). In the Figure, M_0 and Q_0 are bending moment and shear force caused from the part under the surface to the part above the surface, respectively; P_{dyn} and P_{stu} are the hydrodynamic pressure and hydrostatic pressure, respectively; and H_1 is the length of cantilever sheet pile wall part. The calculation of the part under the surface is shown in the calculation model as shown in Figure 4(b). M_0 and Q_0 are bending moment and shear force caused from the part above the surface to the part under the surface, respectively. H_2 is the length of the sheet pile wall into the soil.

3.2. Sheet Pile Wall Stress

(1) R_a is the tension force of the pull rod.

(2) Active earth pressure on the earthquake is P_{E1}. Here, P_{E1} can be calculated using equation (4). The position of dynamic earth pressure joint forces can be calculated using equations (8)–(10).

(3) Due to free water behind the wharf, hydrodynamic pressure joint forces acting in front of the wall can be calculated by Westergaard's method as shown in the following equation:

$$p_{\text{dh}}=\frac{7}{8}\gamma_w k_h\sqrt{h_w h}. \tag{12}$$

Hydrodynamic pressure joint forces can be calculated as shown in the following equation:

$$\begin{aligned}P_{\text{dyn}}&=\int_0^{h_w}P_h dh=\int_0^{h_w}\frac{7}{8}\gamma_w k_h\sqrt{h_w h}dh\\&=\frac{7}{12}\gamma_w k_h h_w^2.\end{aligned} \tag{13}$$

According to the principle of moment equivalence, joint force acting point position was determined, which can be calculated as follows:

$$z_{\text{dw}}=\frac{\int_0^{h_w}(7/8)\gamma_w k_h\sqrt{h_w}\sqrt{h}(h_w-h)dh}{P_{\text{dyn}}}=\frac{2}{5}h_w. \tag{14}$$

(4) Pore water restricted by soil particles, moving along with the soil particles, is called confined water. It produces hydrostatic pressure P_{stu} rather than hydrodynamic pressure. Hydrostatic pressure joint forces can be calculated using equation (16), and hydrostatic pressure force action point can be calculated using equation (20). Free pore water without the restriction of soil particles produces water pressure gradually with the increase of the degree of liquefaction under earthquakes. Wall

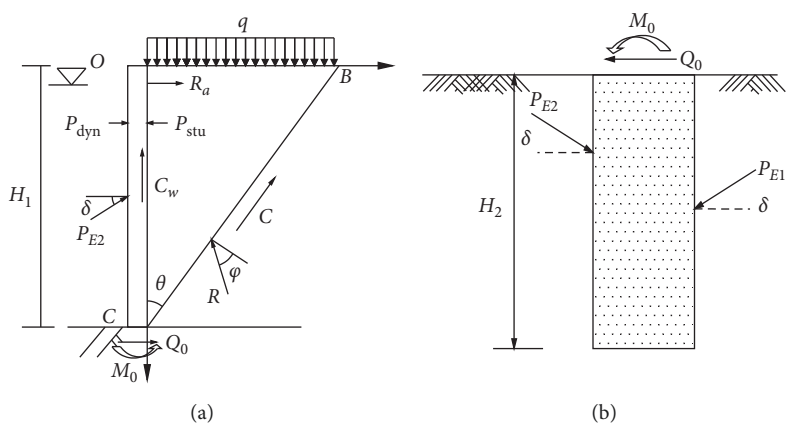

Figure 4: Calculation diagrammatic sketch of front wall's displacement under earthquakes. (a) The front wall above soil surface. (b) The front wall below soil surface.

back water pressure was calculated using the hydrostatic pressure equation without considering liquefaction:

$$p_{sh} = \gamma_w h. \tag{15}$$

Hydrostatic pressure joint forces can be calculated as follows:

$$P_{stu} = \frac{1}{2}\gamma_w h_w^2. \tag{16}$$

Action point position of hydrostatic pressure joint forces can be calculated as follows:

$$z_{sw} = \frac{1}{3}h_w. \tag{17}$$

(5) Shearing force Q_0 located at mud surface from the sheet pile wall can be calculated as follows:

$$\begin{aligned} Q_0 &= -P_{E1}\cos\delta + P_{dyn} + R_a \\ &= -\cos\delta\left\{\frac{m_1}{1-a}\left[(H-h_c)^{1-a} - H_2^{1-a}\right]\right. \\ &\quad \left. + \frac{m_2}{2}\left[H_2^2 - (H-h_c)^2 + m_3(h_c - H_1)\right]\right\} \\ &\quad + \frac{7}{12}\gamma_w K_h h_w^2 + R_a. \end{aligned} \tag{18}$$

(6) Bending moment M_0 located at mud surface from the sheet pile wall can be calculated as follows:

$$\begin{aligned} M_0 &= -P_{E1}z_1\cos\delta + R_a(H_1 - h_0) + P_{dyn}\frac{2}{5}h_w \\ &= -\cos\delta\left\{\frac{m_1}{1-a}\left[(H-h_c)^{1-a} - H_2^{1-a}\right]\right. \\ &\quad \left. + \frac{m_2}{2}\left[H_2^2 - (H-h_c)^2\right] + m_3(h_c - H_1)\right\} \\ &\quad \cdot \left\{\frac{(m_1/(2-a))\left[(H-h_c)^{2-a} - H_2^{2-a}\right] + (m_2/3)\left[H_2^3 - (H-h_c)^3\right] + (m_3/2)\left[H_2^2 - (H-h_c)^2\right]}{(m_1/(1-a))\left[(H-h_c)^{1-a} - H_2^{2-a}\right] + (m_2/2)\left[H_2^2 - (H-h_c)^2\right] + m_3(h_c - H_1)} - H_2\right\} \\ &\quad + R_a(H_1 - h_c) + \frac{7}{30}\gamma_w K_h h_w^3. \end{aligned} \tag{19}$$

(7) Dynamic passive earth pressure P_{E2} on the side of the sea borne by the part in deep soil can be calculated using equation (8). The point position of dynamic passive earth pressure joint forces can be calculated using equations (12)–(14), and overload pressure is calculated as $q = \gamma_w h_w$.

(8) Dynamic active earth pressure P_{E1} on the side of the ground borne by the part in deep soil can be calculated using equation (4), and the point position of dynamic active earth pressure joint forces can be calculated using equations (5)–(7).

3.3. Displacement Calculation for the Lower Part of the Mud Surface of Sheet Pile Wall. Based on mechanics of materials, the deflection curve differential equation of the elastic components part which located at mud surface of the sheet pile wall can be calculated as

$$\mathrm{EI}\frac{d^2y}{dh^2} = -(z_4 + h - H)P_{E4}\cos\delta + (z_3 + h - H)P_{E3}\cos\delta + M_0 + Q_0(h - H_1), \tag{20}$$

where P_{E3} is represented as dynamic active earth pressure joint forces between any part located at mud surface and the part under the mud surface which can be calculated as follows:

$$P_{E3} = \int_{H_1}^{h} p_1 dh = \frac{m_1}{1-a}\left[H_2^{1-a} - (H-h)^{1-a}\right] + \frac{m_2}{2}\left[(H-h)^2 - H_2^2\right] + m_3(H_1 - h), \tag{21}$$

where z_3 is represented as distance from dynamic active earth pressure joint forces, between any part located at mud surface and the part under the mud surface, to the bottom of the wall which can be calculated as follows:

$$z_3 = \frac{\int_{H_1}^{h} p_1(H-h)dh}{\int_{H_1}^{h} p_1 dh} = \frac{(m_1/(2-a))\left[H_2^{2-a} - (H-h)^{2-a}\right] + (m_2/3)\left[(H-h)^3 - H_2^3\right] + (m_3/2)\left[(H-h)^2 - H_2^2\right]}{(m_1/(1-a))\left[H_2^{1-a} - (H-h)^{1-a}\right] + (m_2/2)\left[(H-h)^2 - H_2^2\right] + m_3(H_1 - h)}, \tag{22}$$

where P_{E4} is represented as the dynamic passive earth pressure joint forces between any part located at mud surface and the part under the mud surface which can be calculated as follows:

$$P_{E4} = \frac{m_{p1}}{1-A}\left[H_2^{1-A} - (H-h)^{1-A}\right] + \frac{m_{p2}}{2}\left[(H-h)^2 - H_2^2\right] - m_{p3}(h - H_1), \tag{23}$$

where z_4 is represented as the distance from dynamic passive earth pressure joint forces, between any part located at mud surface and the part under the mud surface, to the bottom of the wall which can be calculated as follows:

$$z_4 = \frac{\int_{H_1}^{h} p_2(H_2 - h + H_1)dh}{\int_{H_1}^{h} p_2 dh} = \frac{(m_{p1}/(2-A))\left[H_2^{2-A} - (H-h)^{2-A}\right] + (m_{p2}/3)\left[(H-h)^3 - H_2^3\right] + (m_{p3}/2)\left[(H-h)^2 - H_2^2\right]}{(m_{p1}/(1-A))\left[H_2^{1-A} - (H-h)^{1-A}\right] + (m_{p2}/2)\left[(H-h)^2 - H_2^2\right] - m_{p3}(h - H_1)}. \tag{24}$$

Boundary conditions are

$$\begin{cases} \varphi_{(h=H)} = 0, \\ y_{(h=H)} = 0. \end{cases} \tag{25}$$

According to the differential solution, the answer is

$$\begin{aligned}\varphi_h = &-\cos\delta m_{p1}\left[\frac{H_2^{2-A}h}{2-A}+\frac{(H-h)^{3-A}}{(2-A)(3-A)}+\frac{H_2^{1-A}h^2}{2(1-A)}+\frac{(H-h)^{2-A}h}{(1-A)(2-A)}+\frac{(H-h)^{3-A}}{(1-A)(2-A)(3-A)}\right.\\&\left.-\frac{HH_2^{1-A}h}{1-A}-\frac{H(H-h)^{2-A}}{(1-A)(2-A)}\right]+\cos\delta m_{p2}\left[\frac{(H-h)^4}{8}+\frac{H_2^3h}{3}+\frac{h(H-h)^3}{6}+\frac{H_2^2h^2}{4}-\frac{H(H-h)^3}{6}-\frac{HH_2^2h}{2}\right]\\&+\cos\delta m_1\left\{\frac{1}{2-a}\left[hH_2^{2-a}+\frac{1}{3-a}(H-h)^{3-a}\right]+\frac{h-H}{1-a}\left[hH_2^{1-a}+\frac{(H-h)^{2-a}}{2-a}\right]-\frac{H_2^{1-a}h^2}{2(1-a)}+\frac{(H-h)^{3-a}}{(1-a)(2-a)(3-a)}\right\}\\&+\cos\delta m_2\left\{-\frac{1}{8}(H-h)^4-\frac{1}{3}H_2^3h+\frac{1}{4}H_2^2h^2+\frac{H-h}{2}\left[\frac{1}{3}(H-h)^3+H_2^2h\right]\right\}+\left(M_0h+\frac{1}{2}Q_0h^2-Q_0H_1h+Q_1\right)\\&+\cos\delta m_3\left[-\frac{(H-h)^3}{6}-\frac{H_2^2h}{2}+\frac{H_1h^2}{2}-\frac{h^3}{3}-H_1Hh+\frac{Hh^2}{2}\right],\end{aligned}\tag{26}$$

$$\begin{aligned}y_h = &\frac{\cos\delta m_{p1}}{\mathrm{EI}}\left\{\frac{1}{2-A}\left[\frac{(H-h)^{4-A}}{(3-A)(4-A)}-\frac{H_2^{2-A}h^2}{2}\right]+\frac{(H-h)^{3-A}(h-H)}{(1-A)(2-A)(3-A)}-\frac{H_2^{1-A}h^3}{6(1-A)}+\frac{2(H-h)^{4-A}}{(1-A)(2-A)(3-A)(4-A)}\right.\\&\left.+\frac{\mathrm{HH}_2^{1-A}h^2}{2(1-A)}\right\}+\frac{\cos\delta m_{p2}}{\mathrm{EI}}\left\{\frac{(H-h)^5}{120}+\frac{H_2^3h^2}{6}+\frac{H_2^2h^3}{12}-\frac{H_2^2Hh^2}{4}\right\}+\frac{\cos\delta m_{p3}}{\mathrm{EI}}\\&\cdot\left[-\frac{(H-h)^4}{24}+\frac{H_2^2h^2}{4}-\frac{Hh^3}{6}+\frac{h^4}{12}-\frac{H_1h^3}{6}+\frac{\mathrm{HH}_1h^2}{2}\right]+\frac{\cos\delta m_1}{\mathrm{EI}}\left\{\frac{1}{2-a}\left[-\frac{(H-h)^{4-a}}{(3-a)(4-a)}+\frac{H_2^{2-a}h^2}{2}\right]+\frac{(h-H)}{1-a}\right.\\&\left.\cdot\left[\frac{H_2^{1-a}h^2}{2}-\frac{(H-h)^{3-a}}{(2-a)(3-a)}\right]-\frac{H_2^{1-a}h^3}{3(1-a)}-\frac{2(H-h)^{4-a}}{(1-a)(2-a)(3-a)(4-a)}\right\}+\frac{\cos\delta m_2}{\mathrm{EI}}\left\{\frac{(H-h)}{2}\left[\frac{(H-h)^5}{60}-\frac{(H-h)^4}{12}\right.\right.\\&\left.\left.+\frac{H_2^2h^2}{2}+\frac{H_2^3h^3}{6}\right]+\frac{(H-h)^5}{40}-\frac{H_2^3h^2}{6}+\frac{H_2^2h^3}{12}\right\}+\frac{\cos\delta m_3}{\mathrm{EI}}\left\{\frac{1}{2}\left[\frac{1}{12}(H-h)^4-\frac{1}{2}H_2^2h^2\right]+\frac{H_1h^3}{6}-\frac{h^4}{12}-\frac{H_1Hh^2}{2}+\frac{Hh^3}{6}\right\}\\&+\frac{1}{\mathrm{EI}}\left(\frac{M_0h^2}{2}+\frac{Q_0h^3}{6}-\frac{Q_0H_1h^2}{2}+Q_1h+Q_2\right),\end{aligned}\tag{27}$$

$$\begin{aligned}Q_1 = &\cos\delta m_{p1}\left(\frac{H_2^{2-A}H}{2-A}-\frac{H_2^{1-A}H^2}{2(1-A)}\right)+\cos\delta m_{p2}\left(\frac{H_2^2H^2}{4}-\frac{H_2^3H}{3}\right)-\cos\delta m_{p3}\left(\frac{H_1H^2}{2}-\frac{H^3}{6}+\frac{H_2^2H}{2}\right)\\&-\cos\delta m_1\left[\frac{1}{2-a}\mathrm{HH}_2^{2-a}-\frac{H_2^{1-a}H^2}{2(1-a)}\right]-\cos\delta m_2\left(-\frac{1}{3}H_2^3H+\frac{1}{4}H_2^2H^2\right)-\cos\delta m_3\left(-\frac{1}{2}\mathrm{HH}_2^2-\frac{1}{2}H_1H^2+\frac{1}{6}H^3\right)\\&-M_0H-\frac{1}{2}Q_0H^2+Q_0H_1H,\end{aligned}\tag{28}$$

$$\begin{aligned}Q_2 = &-\cos\delta m_{p1}\left[\frac{-H_2^{2-A}H^2}{2(2-A)}+\frac{2H_2^{1-A}H^3}{3(1-A)}\right]+\cos\delta m_{p2}\left[\frac{-H_2^3H^2}{6}+\frac{H_2^2H^3}{6}\right]+\cos\delta m_{p3}\left[\frac{-H_2^2H^2}{4}-\frac{H_1H^3}{3}+\frac{H^4}{12}\right]\\&-\cos\delta m_1\left[\frac{H_2^{2-a}H^2}{2(2-a)}-\frac{H_2^{1-a}H^3}{3(1-a)}\right]-\cos\delta m_2\left(\frac{1}{12}H_2^2H^3-\frac{1}{6}H_2^3H^2\right)-\cos\delta m_3\left(-\frac{1}{4}H_2^2H^2-\frac{1}{3}H_1H^3+\frac{1}{12}H^4\right)\\&-\frac{1}{2}M_0H^2-\frac{1}{6}Q_0H^3+\frac{1}{2}Q_0H_1H^2-Q_1H.\end{aligned}\tag{29}$$

3.4. Calculation of the Displacement above the Mud Surface of the Sheet Pile Wall. There are six displacements of the front sheet pile wall, including the displacement caused by mud surface y_0, the one caused by mud corner φ_0, the one caused by dynamic active earth pressure behind the wall Δ, the one caused by tension force f, the one caused by hydrostatic pressure s_s, and the one caused by the hydrodynamic pressure s_d.

(1) Substituting $h = H_1$ in equation (27), then the displacement y_0 of front sheet pile walls located above the mud can be obtained. As is shown in the following equation:

$$y_0 = \frac{\cos\delta m_{p1}}{\mathrm{EI}}\left\{\frac{1}{2-A}\left[\frac{(H_2-H_1)^{4-A}}{(3-A)(4-A)}-\frac{H_2^{2-A}H_1^2}{2}\right]+\frac{H_2}{1-A}\left[\frac{H_2^{1-A}H_1^2}{2}-\frac{(H_2-H_1)^{3-A}}{(2-A)(3-A)}\right]+\frac{H_2^{1-A}H_1^3}{3(1-A)}+\frac{2(H_2-H_1)^{4-A}}{(1-A)(2-A)(3-A)(4-A)}\right\}$$
$$+\frac{\cos\delta m_{p2}}{\mathrm{EI}}\left\{\frac{(H_1-H_2)^5}{30}+\frac{H_2^3H_1^2}{60}-\frac{H_2^2H_1^3}{6}-\frac{1}{2H_2}\left[-\frac{1}{12}(H_2-H_1)^4+\frac{1}{2}H_2^2H_1^2\right]\right\}+\frac{\cos\delta m_{p3}}{\mathrm{EI}}$$
$$\cdot\left[-\frac{(H_2-H_1)^4}{24}+\frac{H_2^2H_1^2}{4}-\frac{\mathrm{HH}_1^3}{6}+\frac{H_1^4}{12}\right]+\frac{\cos\delta m_1}{\mathrm{EI}}\left\{\frac{1}{2-a}\left[-\frac{H_2^{4-a}}{(3-a)(4-a)}+\frac{H_2^{2-a}H_1^2}{2}\right]-\frac{H_2}{1-a}\right.$$
$$\left.\cdot\left[\frac{H_2^{1-a}H_1^2}{2}-\frac{H_2^{3-a}}{(2-a)(3-a)}\right]-\frac{H_2^{1-a}H_1^3}{3(1-a)}-\frac{2H_2^{4-a}}{(1-a)(2-a)(3-a)(4-a)}\right\}+\frac{\cos\delta m_2}{\mathrm{EI}}\left\{\frac{H_2}{2}\left[\frac{H_2^5}{60}-\frac{H_2^4}{12}+\frac{H_2^2H_1^2}{2}+\frac{H_2^3H_1^3}{6}\right]\right.$$
$$\left.+\frac{H_2^5}{40}-\frac{H_2^3H_1^2}{6}+\frac{H_2^2H_1^3}{12}\right\}+\frac{\cos\delta m_3}{\mathrm{EI}}\left\{\frac{1}{2}\left[\frac{1}{12}H_2^4-\frac{1}{2}H_2^2H_1^2\right]+\frac{H_1^4}{12}-\frac{H_1^3H}{3}\right\}+\frac{1}{\mathrm{EI}}\left(\frac{M_0H_1^2}{2}-\frac{Q_0H_1^3}{3}+Q_1H_1+Q_2\right). \tag{30}$$

(2) Substituting $h = H_1$ in equation (26), then the displacement φ_0 of front sheet pile walls located in the angle of the mud can be obtained, as is shown in the following equation:

$$\varphi_0 = -\cos\delta m_{p1}\left\{\frac{1}{2-A}\left[H_1H_2^{2-A}+\frac{(H_2-H_1)^{3-A}}{3-A}\right]-\frac{H_2}{1-A}\left[H_1H_2^{1-A}+\frac{(H_2-H_1)^{2-A}}{2-A}\right]-\frac{H_2^{1-A}H_1^2}{2(1-A)}+\frac{(H_2-H_1)^{3-A}}{(1-A)(2-A)(3-A)}\right\}$$
$$+\cos\delta m_{p2}\left\{\frac{1}{8}(H_2-H_1)^4+\frac{H_1H_2^3}{3}-\frac{H_2^2H_1^2}{4}-\frac{H_2}{2}\left[\frac{1}{3}(H_2-H_1)^3+H_2^2H_1\right]\right\}+\cos\delta m_{p3}\left[\frac{1}{6}(H_2-H_1)^3+\frac{1}{2}H_2^2H_1\right.$$
$$\left.-\frac{1}{2}\mathrm{HH}_1^2+\frac{1}{3}H_1^3\right]+\cos\delta m_1\left\{\frac{1}{2-a}\left[H_1H_2^{2-a}+\frac{1}{3-a}H_2^{3-a}\right]-\frac{H_2}{1-a}\left[H_1H_2^{1-a}+\frac{H_2^{2-a}}{2-a}\right]-\frac{H_2^{1-a}H_1^2}{2(1-a)}+\frac{H_2^{3-a}}{(1-a)(2-a)(3-a)}\right\}$$
$$+\cos\delta m_2\left\{-\frac{1}{8}H_2^4-\frac{1}{3}H_2^3H_1+\frac{1}{4}H_2^2H_1^2+\frac{H_2}{2}\left[\frac{1}{3}H_2^3+H_2^2H_1\right]\right\}+\cos\delta m_3\left[-\frac{H_2^3}{6}-\frac{H_2^2H_1}{2}+\frac{H_1^3}{6}-\frac{H_1^2H}{2}\right]$$
$$+\frac{1}{\mathrm{EI}}\left(M_0H_1-\frac{1}{2}Q_0H_1^2+Q_1\right). \tag{31}$$

(3) The displacement Δ of front sheet pile walls, caused by dynamic active earth pressure behind the wall, can be calculated by using the differential equation as follows:

$$\mathrm{EI}\frac{d^2y}{dh^2} = (z_5+h-H)P_{E5}\cos\delta, \tag{32}$$

where P_{E5} is the represented as dynamic active earth pressure joint forces in any depth of the wharf surface, which can be calculated as follows:

$$P_{E5} = \int_{h_c}^{h} p_1 dh = \frac{m_1}{1-a}\left[(H-h_c)^{1-a}-(H-h)^{1-a}\right]$$
$$+\frac{m_2}{2}\left[(H-h)^2-(H-h_c)^2\right]+m_3(h_c-h), \tag{33}$$

where z_5 is represented as the distance between the function point of dynamic active earth pressure joint forces in any depth of the wharf surface and the bottom of the wall which can be calculated as follows:

$$z_5 = \frac{\int_{h_c}^{h} p_1 (H-h)dh}{\int_{h_c}^{h} p_1 dh} = \frac{\left(\left(m_1\left[(H-h_c)^{2-a}-(H-h)^{2-a}\right]\right)/(2-a)\right)+\left(\left(m_2\left[(H-h)^3-(H-h_c)^3\right]\right)/3\right)+\left(\left(m_3\left[(H-h)^2-(H-h_c)^2\right]\right)/2\right)}{(m_1/(1-a))\left[(H-h_c)^{1-a}-(H-h)^{1-a}\right]+(m_2/2)\left[(H-h)^2-(H-h_c)^2\right]+m_3(h_c-h)}. \tag{34}$$

Boundary conditions are

$$\begin{cases} \varphi_{(h=H_1)} = \dfrac{dy}{dh}_{(h=H_1)} = 0, \\ y_{(h=H_1)} = 0. \end{cases} \tag{35}$$

The answer is

$$\begin{aligned} \Delta = y = {} & \frac{m_1 \cos\delta}{\mathrm{EI}}\left[\frac{(H-h_c)^{2-a}h^2}{2(2-a)} - \frac{(H-h)^{4-a}}{(4-a)(3-a)(2-a)} - \frac{(H-h_c)^{1-a}(H-h)^3}{6(1-a)} + \frac{(H-h)^{4-a}}{(1-a)(3-a)(4-a)}\right] \\ & + \frac{m_2 \cos\delta}{\mathrm{EI}}\left[-\frac{(H-h)^5}{120} - \frac{(H-h_c)^3 h^2}{6} + \frac{(H-h_c)^2(H-h)^3}{12}\right] \\ & + \frac{m_3 \cos\delta}{\mathrm{EI}}\left[\frac{(H-h)^4}{24} - \frac{(H-h_c)^2 h^2}{2} - \frac{h_c(H-h)^3}{6} + \frac{Hh^3}{6}\right] + \frac{\cos\delta}{\mathrm{EI}}(Q_1 h + Q_2), \end{aligned} \tag{36}$$

$$\begin{aligned} Q_1 = {} & m_1\left[\frac{-1}{2-a}(H-h_c)^{2-a}H_1 - \frac{H_2^{3-a}}{(3-a)(2-a)} - \frac{(H-h_c)^{1-a}H_2^2}{2(1-a)} + \frac{H_2^{3-a}}{(3-a)(1-a)}\right] \\ & + m_2\left[-\frac{1}{24}H_2^4 + \frac{1}{3}(H-h_c)^3 H_1 + \frac{1}{4}(H-h_c)^2 H_2^2\right] \\ & + m_3\left[\frac{H_2^3}{6} + \frac{(H-h_c)^2 H_1}{2} - \frac{h_c H_2^2}{2} + \frac{H_1^3}{3} - \frac{\mathrm{HH}_1^2}{2}\right], \end{aligned} \tag{37}$$

$$\begin{aligned} Q_2 = {} & m_1\left[\frac{-(H-h_c)^{2-a}H_1^2}{2(2-a)} + \frac{H_2^{4-a}}{(4-a)(3-a)(2-a)} + \frac{(H-h_c)^{1-a}H_2^3}{6(1-a)} - \frac{H_2^{4-a}}{(1-a)(4-a)(3-a)}\right] \\ & + m_2\left[\frac{H_2^5}{120} + \frac{(H-h_c)^3 H_1^2}{6} - \frac{(H-h_c)^2 H_2^3}{12}\right] + m_3\left[-\frac{H_2^4}{24} + \frac{(H-h_c)^2 H_1^2}{2} + \frac{H_2^3 h_c}{6} + \frac{H_1^4}{12} - \frac{\mathrm{HH}_1^3}{6}\right] \\ & - Q_1 H_1. \end{aligned} \tag{38}$$

(4) Based on material mechanics equations, the displacement f of front sheet pile walls caused by tension force is

$$M_h = \mathrm{EI}\frac{d^2 y}{dh^2} = R_a(h-h_0). \tag{39}$$

Boundary conditions are

$$\begin{cases} \varphi_{(h=H_1)} = 0, \\ y_{(h=H_1)} = 0. \end{cases} \tag{40}$$

The answer is

$$\begin{aligned} f = y = {} & \frac{R_a h^3}{6\mathrm{EI}} - \frac{R_a h_0 h^2}{2\mathrm{EI}} \\ & + \frac{2R_a h_0 H_1 h - R_a H_1^2 h}{2\mathrm{EI}} \\ & + \frac{2R_a H_1^3 - 3R_a h_0 H_1^2}{6\mathrm{EI}}. \end{aligned} \tag{41}$$

(5) Based on material mechanics equations, the displacement s_s of front sheet pile walls caused by hydrostatic pressure is

$$M_h = \mathrm{EI}\frac{d^2 y}{dh^2} = \frac{1}{6}\gamma_w\left[h-(H_1-h_w)\right]^3. \tag{42}$$

Boundary conditions are

$$\begin{cases} \varphi_{(h=H_1)} = 0, \\ y_{(h=H_1)} = 0. \end{cases} \tag{43}$$

The answer is

$$s_s = y = \frac{\gamma_w}{120\mathrm{EI}}\left[h - (H_1 - h_w)\right]^5 + \frac{C_1}{\mathrm{EI}}h + \frac{C_2}{\mathrm{EI}}, \tag{44}$$

where:

$$C_1 = -\frac{\gamma_w}{24}h_w^4, \quad C_2 = \frac{\gamma_w}{24}h_w^4 H_1 - \frac{\gamma_w}{120}h_w^5. \tag{45}$$

(6) Based on the material mechanics equations, the displacement s_d of front sheet pile walls caused by hydrodynamic pressure is

$$M_h = \mathrm{EI}\frac{d^2 y}{dh^2} = \frac{7}{30}\gamma_w K_h \cdot \sqrt{h_w}\left(h - H_1 + h_w\right)^{(5/2)}. \tag{46}$$

Boundary conditions are

$$\begin{cases} \varphi_{(h=H_1)} = 0, \\ y_{(h=H_1)} = 0. \end{cases} \tag{47}$$

The answer is

$$s_d = y = \frac{2\gamma_w K_h}{135\mathrm{EI}}\sqrt{h_w}\left(h - H_1 + h_w\right)^{(9/2)} + \frac{C_1}{\mathrm{EI}}h + \frac{C_2}{\mathrm{EI}}, \tag{48}$$

where

$$C_1 = -\frac{\gamma_w K_h}{15}h_w^4, \quad C_2 = \frac{\gamma_w}{15}K_h h_w^4 H_1 - \frac{2\gamma_w K_h}{135}h_w^5. \tag{49}$$

Displacement of any points above the mud surface of the front sheet pile walls can be expressed as

$$y_h = y_0 + \varphi_0\left(H_1 - h\right) + \Delta_h + f_h + s_{\mathrm{sh}} + s_{\mathrm{dh}}. \tag{50}$$

Substituting (30), (31), (36), (41), (44), and (48) in equation (50), the solution of displacement of any points above the mud surface of the front sheet pile walls under the earthquake function can be obtained.

In equation (50), except for conditions that have been known, tension force R_a can be calculated by assuming the displacement located at the anchor point of the sheet pile walls, and by analyzing the results of finite element calculation and that of dynamic test, the deformation characteristics of the sheet pile wall can be obtained. The anchor point displacement in this paper is assumed as the following equation:

$$y_{h=h_0} = \frac{y_0\left(H - h_0\right)}{H_2}. \tag{51}$$

Substituting $h = h_0$ from equation (50) in equation (51), the value of tension force R_a can be obtained.

4. Engineering Example

4.1. Engineering Survey. The model is based on a practical engineering example. The structures of the front wall and anchor wall are the underground continuous walls. Front wall thickness is 0.8 m and buried depth is 8 m; anchor wall thickness is 1 m, the height is 4 m, and cover filling is 2 m; distance between front wall and anchorage wall is 10 m; and diameter of rod is 6 cm, and depth of sea is 6 m. The section is shown in Figure 5. Load of the wharf surface is 20 kN/m. The Kobe wave is the seismic load wave, and the waves of horizontal and vertical are loading at the same time. Maximum horizontal acceleration amplitude is 0.1 g; maximum vertical acceleration amplitude is 0.05 g. The waveform is shown in Figure 6. The soil was assumed to be a single soil layer in the process of deriving the sheet pile wharf displacement calculation theory; hence, the single soil layer can be chosen in finite element analysis.

In order to verify the rationality of the calculation method, some working conditions of increasing the internal friction and angle cohesion and reducing the elastic modulus of backfill soils were studied and the related parameters of soils are listed in Table 1. The calculated values are compared with the numerical simulation values. The parameters of the anchor wall, sheet pile wall, and bar are also shown in Table 1.

4.2. Theoretical Calculation Results. According to the theoretical calculation of the sheet pile quay wall under earthquakes, displacement calculation data are shown in Table 2. Table 3 lists the symbols in Table 2.

The unit of force is kN, the unit of length is m, and the unit of moment is kN·m.

4.3. Comparative Analysis of Calculation Results. The calculation of front sheet pile wall displacement theory and finite element calculation results under the earthquake function are shown in Figure 7. These two calculation methods are close under the mud and have a little error in the calculation of displacement of the front wall above the mud. The maximum displacement of the front wall occurs at about the height of 12 meters of the front wall when using

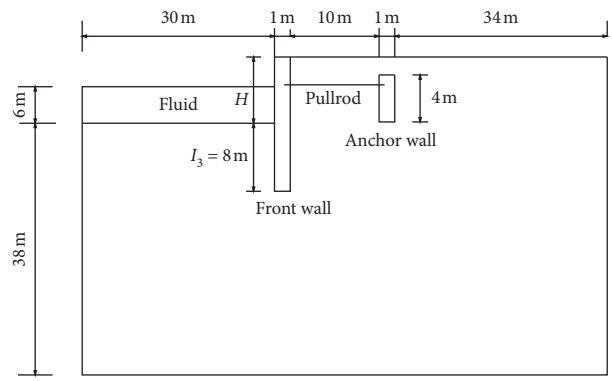

Figure 5: Diagram of the calculation model.

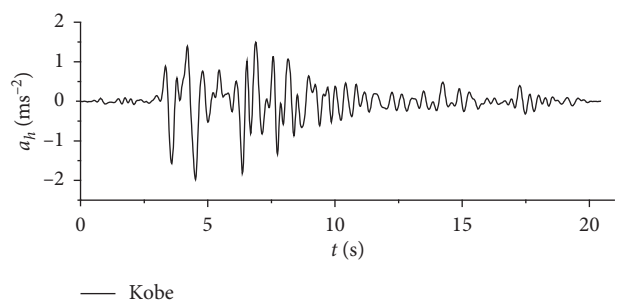

Figure 6: Input earthquake motion.

Table 1: Parameters of soil mass, wall, and drawbar material.

Material type	Working condition	Unit weight (kN/m^3)	Internal friction angle (°)	Cohesion (kPa)	Elastic modulus (MPa)	Poisson's ratio
Layer 1	①	19.1	27.0	20	8.97	0.30
Layer 1	②	19.1	35.0	20	8.97	0.30
Layer 1	③	19.1	27.0	20	8.97	0.30
Layer 1	④	19.1	27.0	30	4.00	0.30
Concrete		25.0	—	—	2.8×10^4	0.20
Steel tie rod		78.5	—	—	2.06×10^5	0.20

theoretical equations. The maximum displacement of the front wall occurs at the top of the front wall when using finite element software.

For the four working conditions, the displacement of the front wall decreases with increase in the internal friction angle and cohesion and increases with decrease in the elastic modulus of backfill soils. All displacements do not exceed the permission displacement which is 1% of the whole wall height. The research results show that the calculation method of seismic residual displacement on sheet pile quay walls is reasonable for different cases.

The pseudostatic method can be applied during the calculation process of the theoretical equations, which can reflect the dynamic characteristics of load but cannot reflect the dynamic response of various materials and dynamic coupling relationship between the structures. The proportional displacement method is applied when determining the value of tension force; hence, the results may have errors. In this example, the results of tension force are relatively big, which lead to the displacement of the front wall be small, and the front wall convex drum is obvious.

5. Conclusions

Based on the pseudostatic method and the calculation method for obtaining the dynamic earth pressure of clay soil, combining structural characteristics of sheet pile quay wall, and differential equation of deflection line, the calculating formula of the front wall's seismic residual displacement for the sheet pile wharf is derived.

Due to the lack of front wall displacement test data of the sheet pile quay wall under earthquakes at the present, comparison is made between the theoretical results and the ADINA simulation results to prove the effectiveness of the theoretical equation. Comparison results show that these

Table 2: Calculation data of front wall's displacement.

Ignoring the anchor point displacement		Considering the anchor point displacement	
Variable	Value	Variable	Value
k_h	0.10	n_{p1}	2.359
k_v	0.05	n_{p2}	−0.776
h_w	6.00	n_{p3}	−3.084
η	6.011	m_{p1}	1062.866
n_1	0.403	m_{p2}	31.788
n_2	−0.761	m_{p3}	65.649
n_3	−1.535	A	0.354
I_1	140.231	B	17.943
I_2	47491.034	I_{p1}	108.474
I_3	5844.779	I_{p2}	11949.382
θ_1	40.398	I_{p3}	2486.645
h_c	2.090	θ_2	68.449
a	0.024	R_a	365.116
b	−10.880	Q_0	−266.251
m_1	−63.642	M_0	−2004.722
m_2	7.181	y_0	−0.033
m_3	−159.633	φ_0	0.0178
q_1	−59.919	q_2	60
The front wall displacement equations of part above the mud		The front wall displacement equations of part under the mud	
$y = -3.598 \times 10^{-7}(16-h)^{3.646} + 1.792 \times 10^{-4}h^2 - 5.392 \times 10^{-6}h^3 + 5.043 \times 10^{-10}(16-h)^5 + 6.520 \times 10^{-8}h^4 - 3.260 \times 10^{-8}(16-h)^4 - 9.680 \times 10^{-9}(16-h)^{3.976} + 2.268 \times 10^{-3}h + 2.079 \times 10^{-10}(16-h)^6 + 1.261 \times 10^{-6}(16-h)h^2 + 1.064 \times 10^{-6}(16-h)h^3 - 0.0647$		$y = 3.099 \times 10^{-3}h^2 - 9.686 \times 10^{-7}(16-h)^{3.976} + 0.0219h + 1.088 \times 10^{-4}(16-h)^3 - 2.079 \times 10^{-8}(16-h)^5 - 1.261 \times 10^{-4}h^3 - 2.31 \times 10^{-6}(16-h)^4 + 0.0178(8-h) + 1.286 \times 10^{-8}(h-2)^{4.5} - 0.384$	

Table 3: The symbols in Table 2.

k_h	The horizontal seismic coefficient
k_v	The vertical seismic coefficient
h_w	Depth of water
η	Seismic angle
n_1	$n_1 = ((\cos(\theta+\varphi-\eta))/\cos\theta) . ((\cos\theta\sin\eta - \sin(\theta-\eta))/(\sin\delta\cos(\theta+\varphi-\eta) - \sin(\theta+\varphi)\cos(\delta+\eta)))$
n_2	$n_2 = ((\cos(\theta+\varphi-\eta) + \sin(\theta+\varphi)\sin\eta)/(\sin\delta\cos(\theta+\varphi-\eta) - \sin(\theta+\varphi)\cos(\delta+\eta)))$
n_3	$n_3 = (1/\cos\theta)\cdot(\cos\eta\cos\varphi/(\sin\delta\cos(\theta+\varphi-\eta) - \sin(\theta+\varphi)\cos(\delta+\eta)))$
I_1	$I_1 = (\cos\delta/(\cos^2(\varphi+\delta)))[(1/2)\gamma(H-h_c)((1-k_v)/\cos\eta)\sin(\varphi-\eta) + (q+\gamma h_c)((1-k_v)/\cos\eta)\sin(\varphi-\eta) + c\cos\varphi]$
I_2	$I_2 = ((H-h_c)^2/\cos\delta\cos^2(\varphi+\delta))\cdot[(1/2)\gamma(H-h_c)((1-k_v)/\cos\eta)\sin(\varphi+\delta)\cos(\delta+\eta) + c_w\cos\varphi\cos(\delta+\varphi) + c\cos\varphi + (q+\gamma h_c)((1-k_v)/\cos\eta)\sin(\delta+\varphi)\cos(\delta+\eta)]$
I_3	$I_3 = \{[(1/2)\gamma(H-h_c)((1-k_v)/\cos\eta) + (q+\gamma h_c)((1-k_v)/\cos\eta)]\cdot[\sin(\varphi+\delta)\sin(\varphi-\eta) + \cos(\delta+\eta)] + 2c\cos\varphi\sin(\varphi+\delta) + c_w\sin\varphi\cos(\varphi+\delta)\}((H-h_c)/(\cos^2(\varphi+\delta)))$
θ_1	θ_1 is the rupture angle when neglecting the displacement of anchorage point
h_c	The depth of crack: $h_c = ((n_2c_w\cos\eta - n_3c\cos\eta - n_1q(1-k_v))/(n_1\gamma(1-k_v)))$
a	$a = 1 - n_1((\cos\theta\sin(\theta+\varphi+\delta))/(\cos(\theta+\varphi-\eta)\sin\theta))$
b	$b = ((2[c_w\sin(\theta+\varphi)\cos\delta\cos\theta - c\cos\varphi\cdot\sin\delta])/(\sin\theta[\sin\delta\cos(\theta+\varphi-\eta) - \sin(\theta+\varphi)\cos(\delta+\eta)]))$
m_1	$m_1 = n_1(\gamma((1-k_v)/(\cos\eta))((H-h_c)/(1+a)) + (b/a) + ((1-k_v)/\cos\eta)q_1)(H-h_c)^a$
n_{p1}	$n_{p1} = ((\cos(\theta+\eta-\varphi))/\cos\theta)\cdot(\cos\theta\sin\eta + \sin(\theta+\eta)/(\sin\delta\cos(\theta-\varphi+\eta) + \sin(\theta-\varphi)\cos(\delta+\eta)))$
n_{p2}	$n_{p2} = -((\cos(\theta+\eta-\varphi) - \sin(\theta-\varphi)\sin\eta)/(\sin\delta\cos(\theta-\varphi+\eta) + \sin(\theta-\varphi)\cos(\delta+\eta)))$
n_{p3}	$n_{p3} = -(1/\cos\theta)\cdot((\cos\eta\cos\varphi)/(\sin\delta\cos(\theta-\varphi+\eta) + \sin(\theta-\varphi)\cos(\delta+\eta)))$
m_{p1}	$m_{p1} = n_{p1}(\gamma((1-k_v)/\cos\eta)(H/(1+A)) + (B/A) + ((1-k_v)/\cos\eta)q)H^A$
m_{p2}	$m_{p2} = n_{p1}\gamma((1-k_v)/\cos\eta)(1/(1+A))$
m_{p3}	$m_{p3} = n_{p1}(B/A) - n_{p2}c_w + n_{p3}c$
A	$A = 1 - n_{p1}((\cos\theta\sin(\theta-\varphi-\delta))/(\cos(\theta+\eta-\varphi)\sin\theta))$
B	$B = ((2[c\cos\varphi\sin\delta + c_w\sin(\theta-\varphi)\cdot\cos\delta\cos\theta])/(\sin\theta[\sin\delta\cdot\cos(\theta-\varphi+\eta) + \sin(\theta-\varphi)\cos(\delta+\eta)]))$
I_{p1}	$I_{p1} = (\cos\delta/(\cos^2(\delta+\varphi)))\cdot[(1/2)\gamma H((1-k_v)/\cos\eta)\sin(\varphi-\eta) + q((1-k_v)/\cos\eta)\sin(\varphi-\eta) + c\cos\varphi]$
I_{p2}	$I_{p2} = (H^2/(\cos\delta\cos^2(\varphi+\delta)))\cdot[(1/2)\gamma H((1-k_v)/\cos\eta)\sin(\delta+\varphi)\cos(\delta+\eta) + q((1-k_v)/\cos\eta)\cdot\sin(\delta+\varphi)\cos(\delta+\eta) + c\cos\varphi + c_w\cos\delta\cos(\delta+\varphi)]$
I_{p3}	$I_{p3} = (H/(\cos^2(\varphi+\delta)))\cdot\{((1/2)\gamma H((1-k_v)/\cos\eta) + q((1-k_v)/\cos\eta))[\sin(\varphi+\delta)\sin(\varphi-\eta) + \cos(\delta+\eta)] + 2c\cos\varphi\cdot\sin(\varphi+\delta) + c_w\sin\varphi\cos(\varphi+\delta)\}$
θ_2	θ_2 is the rupture angle when considering the displacement of anchorage point
R_a	The tension force of pull rod
Q_0	The shear force caused by the part under the surface to the part above the surface
M_0	The bending moment caused by the part under the surface to the part above the surface

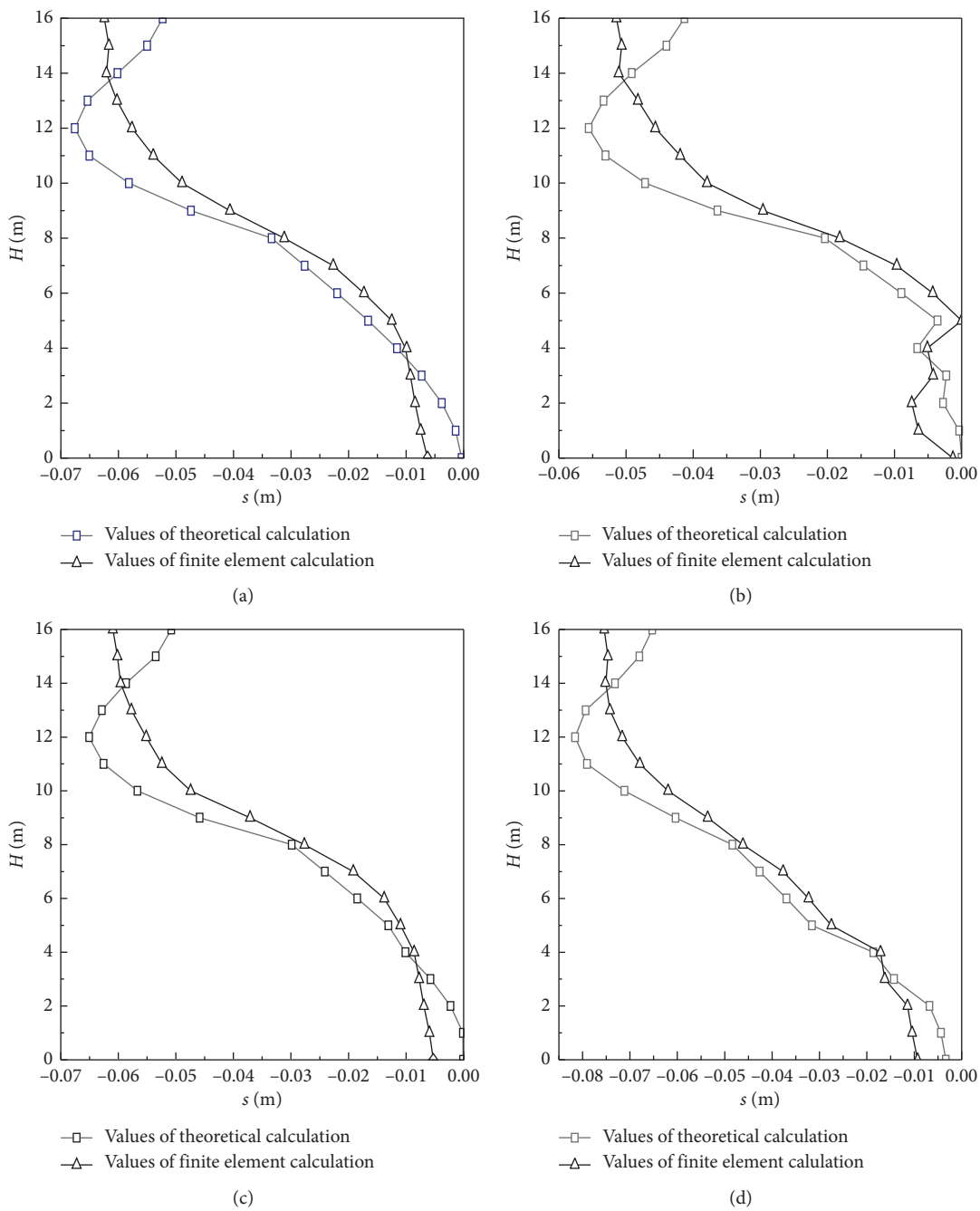

Figure 7: Comparison between calculation results of displacement for theoretical method and FE method. Working condition: (a) ①; (b) ②; (c) ③; (d) ④.

two calculation methods are close under the mud, but they have little difference in the calculation results of displacement of the front wall above the mud because of the proportional displacement method which leads to the displacement of the front wall in the tie rod have little difference within the acceptable range. In this paper, the front wall displacement equation of the sheet pile quay wall under seismic loads has been derived which has higher precision and certain practical reference value.

Data Availability

The data used to support the findings of this study are available from the corresponding author upon request.

Conflicts of Interest

The authors declare that there are no conflicts of interest regarding the publication of this paper.

Acknowledgments

This research was financially supported by the Natural Science Foundation of Jiangsu Province (Grant no. BK20161360), Six Major Talents Peak in Jiangsu Province in China (Grant no. 2016-JZ-020), and Postgraduate Research & Practice Innovation Program of Jiangsu Province (Grant no. KYCX19_1702).

References

[1] J. Zhang and J. X. Gong, "Comparative analysis on seismic design approach of sheet pile wharf in China, the U.S. and Japan," *Waterway Engineering*, vol. 445, no. 9, pp. 136–154, 2010.

[2] S. R. Christie, "Seismic design methods for anchored sheet pile bulkheads ports," in *Proceedings of the Building on the Past, Respecting the Future*, American Society of Civil Engineers, Jacksonville, FL, USA, April 2010.

[3] G. Gazetas, E. Garini, and A. Zafeirakos, "Seismic analysis of tall anchored sheet-pile walls," *Soil Dynamics and Earthquake Engineering*, vol. 91, pp. 209–221, 2016.

[4] A. Zekri, A. Ghalandarzadeh, P. Ghasemi, and M. H. Aminfar, "Experimental study of remediation measures of anchored sheet pile quay walls using soil compaction," *Ocean Engineering*, vol. 93, pp. 45–63, 2015.

[5] C. W. Yu, C. J. Lee, W. Y. Hung, and H. T. Chen, "Application of Hilbert-Huang transform to characterize soil liquefaction and quay wall seismic responses modeled in centrifuge shaking-table tests," *Soil Dynamics and Earthquake Engineering*, vol. 30, no. 7, pp. 614–629, 2010.

[6] H. H. Lee and P. Y. Chang, "The damage inspection and safety assessment on steel-sheet pile wharf structural system," *Fracture and Damage Mechanics V*, vol. 324-325, pp. 1221–1224, 2006.

[7] D. Choudhury and S. M. Ahmad, "Stability of waterfront retaining wall subjected to pseudo-static earthquake forces," *Ocean Engineering*, vol. 34, no. 14-15, pp. 1947–1954, 2007.

[8] Y. Tan and Y. Lu, "Parametric studies of DDC-induced deflections of sheet pile walls in soft soils," *Computers and Geotechnics*, vol. 36, no. 5, pp. 902–910, 2009.

[9] R. Motamed and I. Towhata, "Mitigation measures for pile groups behind quay walls subjected to lateral flow of liquefied soil: shake table model tests," *Soil Dynamics and Earthquake Engineering*, vol. 30, no. 10, pp. 1043–1060, 2010.

[10] X. Wang, "FEM analysis of the corrosion residual bearing capacity of steel sheet piles link-banked structure of high-piled wharf," in *Proceedings of the International Conference on Computer Engineering and Technology*, pp. 113–117, Chengdu, China, April 2010.

[11] Ö. Bilgin, "Numerical studies of anchored sheet pile wall behavior constructed in cut and fill conditions," *Computers and Geotechnics*, vol. 37, no. 3, pp. 399–407, 2010.

[12] L. Y. Wang, X. X. Chen, and H. L. Liu, "Effective stress study of seismic residual deformations of caisson quay wall in liquefied foundation earthquake," *Rock and Soil Mechanics*, vol. 32, no. 11, pp. 3361–3367, 2011.

[13] L. Y. Wang, Y. Cai, and H. L. Liu, "Validation of calculation method for the seismic residual deformation of gravity quays in liquefied foundation by dynamic tests," *China Civil Engineering Journal*, vol. 44, no. 10, pp. 113–117, 2011.

[14] L. Y. Wang, S. K. Chen, and P. Gao, "Research on seismic internal forces of geogrids in reinforced soil retaining wall structures under earthquake actions," *Journal of Vibroengineering*, vol. 16, no. 4, pp. 2023–2034, 2014.

[15] L. Wang, G. Chen, and S. Chen, "Experimental study on seismic response of geogrid reinforced rigid retaining walls with saturated backfill sand," *Geotextiles and Geomembranes*, vol. 43, no. 1, pp. 35–45, 2015.

[16] L. Y. Wang, G. X. Chen, P. Gao, and S. K. Chen, "Pseudostatic calculation method of the seismic residual deformation of a geogrid reinforced soil retaining wall with a liquefied backfill," *Journal of Vibroengineering*, vol. 17, no. 2, pp. 827–840, 2015.

[17] L.-Y. Wang, H.-L. Liu, P.-M. Jiang, and X.-X. Chen, "Prediction method of seismic residual deformation of caisson quay wall in liquefied foundation," *China Ocean Engineering*, vol. 25, no. 1, pp. 45–58, 2011.

[18] W.-X. Chen, L.-Y. Wang, J. Li, and B.-H. Wang, "Displacement calculation method on front wall of covered sheet-pile wharf," *Advances in Civil Engineering*, vol. 2018, Article ID 5037057, 13 pages, 2018.

[19] J.-S. Chiou, C.-H. Chiang, H.-H. Yang, and S.-Y. Hsu, "Developing fragility curves for a pile-supported wharf," *Soil Dynamics and Earthquake Engineering*, vol. 31, no. 5-6, pp. 830–840, 2011.

[20] Z. K. Cheng, D. G. Wang, Y. C. Ding, and J. Z. Hang, "Analysis of waterfront excavation adjacent to pile-supported wharves," *New Frontiers in Engineering Geology and the Environment*, pp. 53–56, Springer, New York, NY, USA, 2013.

[21] L. Wang, J. Yan, W. Gong, Q. Wang, and B. Wang, "Dynamic shear properties of recycled waste steel slag used as a geo-backfill material—revised version," *Shock and Vibration*, vol. 5, pp. 1–17, 2019.

[22] L. Wang, J. Yan, Q. Wang, B. Wang, and A. Ishimwe, "Study on permeability of steel slag and steel slag modifying silt soil as geo-materials," *Advances in Civil Engineering*, vol. 2019, Article ID 5370748, 2019.

[23] Y. Lin, G. Yang, L. Zhao, and Z. Zhong, "Horizontal slices analysis method for seismic earth pressure calculation," *Chinese Journal of Rock Mechanics and Engineering*, vol. 29, no. 12, pp. 2581–2591, 2010.